

Implementation of Sensitivity and Resolution Modeling for SPECT with Cone-Beam Collimator

A. Krol^{*a}, V. R. Kunniyur^b, W. Lee^a, K. R. Gangal^b, I. L. Coman^c, E. D. Lipson^d,
D. A. Karczewski^a, F. D. Thomas^a, D. H. Feiglin^a

^aSUNY Upstate Medical University, Department of Radiology, Syracuse, NY13210, USA;

^bSyracuse University, Department of Electrical Engineering and Computer Science, Syracuse, NY, USA; ^cIthaca College, Department of Mathematics and Computer Science, Ithaca, NY, USA;

^dSyracuse University, Department of Physics, Syracuse, NY, USA;

ABSTRACT

We implemented a fully-3D ordered subsets expectation maximization (OSEM) algorithm with compensation of attenuation, distance-dependent blurring (DDB) and sensitivity modeling for SPECT performed with cone-beam collimator (CBC). The experimentally obtained detector response to point sources across FOV was fitted to a two-dimensional Gauss function with its width (FWHM) varied linearly with the source-to-detector distance and with very weak sensitivity dependence on the emission angle. We obtained CBC SPECT scans of a physical point source phantom, Defrise phantom and a female patient, and investigated performance of our algorithm. Our studies indicated that to correctly simulate DDB and sensitivity a blurring kernel with a radius of up to 10 elements had to be used for 128x128 acquisition matrix and volumetric ray tracing rather than line element based ray tracing has to be implemented. In the point source phantom reconstruction we evaluated the uniformity of FWHM for the radial, tangential and longitudinal directions, and sensitivity vs. distance. An isotropic and stationary resolution was obtained at any location by OSEM with DDB and sensitivity modeling only when volumetric ray tracing was utilized. We analyzed axial and transaxial profiles obtained for Defrise phantom and evaluated the reconstructed breast SPECT patient images. The proposed fully-3D OSEM reconstruction algorithm with DDB and sensitivity modeling, and attenuation compensation with volumetric rays tracing is efficient and effective with significant resolution and sensitivity recovery.

Keywords: Cone-beam SPECT, resolution modeling, sensitivity modeling, ray trace

1. INTRODUCTION

Cone-beam SPECT can be used to improve the trade-off between sensitivity and resolution for small organs that fit in the tomographic field of view of a cone-beam collimator (CBC). This technique requires fully -3D reconstruction with resolution and sensitivity modeling, and is hindered by artifacts in the non-central slices. These artifacts might be caused by truncation and by the fact that cone-beam SPECT data collected in a circular orbit contain insufficient information for exact reconstruction of non-central slices. Additional artifacts might originate from the errors in the estimation of the system transition matrix. In this paper we investigate a method for improved 3D iterative reconstruction that approximates volumetric ray tracing via ray trace with multiple rays per detector bin in order to better estimate the elements of the system matrix, as compared to a single ray trace per detector bin approach. In both cases the Siddon's algorithm (Siddon 1985) for the line element ray trace that was used and a fully-3D ordered subsets EM (OSEM) algorithm was implemented with compensation of attenuation and distance-dependent blurring (DDB) and sensitivity modeling for CBC SPECT.

* krola@upstate.edu ; tel. 315 464 7054; fax 315 464 7068

The experimentally obtained detector response to point sources across FOV was fitted to a two-dimensional Gauss function with its width (FWHM) varied linearly with the source-to-detector distance and with very weak sensitivity dependence on the emission angle.

2. MATERIALS AND METHODS

We acquired projection images of “point” sources vs. distance. Nine sources were fixed on a thin plastic plate in pattern that assured the same emission angle (Fig. 1). Each source contained approximately 1 μCi of Tc-99m and the distance from the collimator face to the source was varied in the 5 – 40 cm range. The planar images were acquired with E.Cam (Siemens Medical Systems) gamma camera in 512 \times 512 matrix and 5 minutes per image. Cone beam collimator (Nuclear Fields) with $f=70$ cm focal length was used. Multiple line profiles through the images of “point” sources were obtained and fitted to a Gauss function.

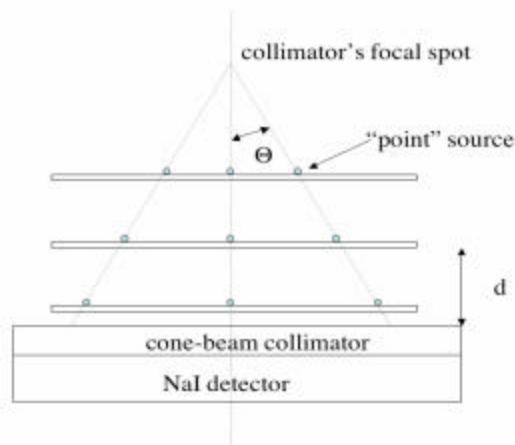


Fig. 1. Geometry of “point” sources projection images acquisition with cone beam collimator and identical emission angle Θ vs. d , the distance from the collimator face.

We performed SPECT scans (90 views in 360° circular orbit, ROR=24cm, 25 sec/view) of a DeFrise phantom filled with 0.9 $\mu\text{Ci/ml}$ of Tc-99m using a dual-head gamma camera (E.Cam, Siemens) equipped with one high-resolution cone-beam ($f = 70$ cm) and one high-resolution parallel-beam collimator. The cone-beam SPECT reconstructions were initiated from tomographic images obtained using OSEM of the PBC SPECT data [1-2].

A small number of patients with suspicious breast lesions were administered 10 mCi of Tc-99m sestamibi. SPECT Tc-99m sestamibi scintimammography (90 views, 30 sec/view, parallel-hole high-resolution collimator) was acquired on a dual-head gamma camera (E.Cam, Siemens). In addition, in order to simulate hot breast lesions, some patients were imaged with a number of breast skin markers each containing 1 μCi of Tc-99m.

The images were reconstructed using a maximum-likelihood expectation-maximization algorithm (MLEM)²⁻³ in its ordered subset version⁴⁻⁵. We performed fully-3D reconstruction with resolution and attenuation modeling. We used our version of an MLEM algorithm⁶:

$$I_k^{n+1} = I_k^n \frac{1}{\sum_{i \in S_0} c_{ik}} \sum_{i \in S_0} \left\{ c_{ik} \cdot \mathbf{g}_{ij} \frac{Y_i}{\sum_{m \in P_i} I_m^n \cdot c_{im} \cdot \mathbf{g}_{ij}} + c_{ik}(1 - \mathbf{g}_{ij}) \right\} \quad (1)$$

The symbols are as follows:

- i projection subscript,
- J_i number of pixels in the ray I
- j pixel subscript ($j < J_i$),
- P_i set of pixels contributing to projection i ,
- S_0 subset of the projection bins corresponding to a particular set of views,
- R_{k0} subset of projections that belongs to S_0 to which pixel k contributes,
- Y_i total (random) number of photons recorded by the detector bin i ,
- I_j^n current estimate of source intensity of pixel j (*i.e.* the mean number of photons emitted by pixel j),
- μ_j linear attenuation coefficient of pixel j ,
- l_{ij} the length of intersection of the pixel j , *i.e.* the fraction of the ray originated from the center of detector bin i intercepted by pixel j
- \mathbf{g}_{ij} probability of surviving attenuation between the source in the pixel j for the photon heading towards the detector bin i , c_{ij} known probability (corrected for the decay rate and the time interval of i th projection) that photon leaving pixel j is directed toward detector bin i .

The summation in (1) is performed over a subset S_0 of the projection bins corresponding to a particular set of views. The images are updated after a user-specified number of projection views (OS size) that form the subset S_0 . The OS size may vary from unity (the smallest possible) to the number of acquired views (the largest possible).

3. RESULTS

In the “point” sources reconstruction we evaluated the uniformity of spatial resolution, *i.e.* FWHM of the Gaussian function fit to the line profiles through the planar images of the sources for the radial, tangential and longitudinal directions vs. distance (not shown) and sensitivity, *i.e.* total number of counts recorded by a gamma camera equipped with a cone beam collimator, vs. distance (Fig. 2). An isotropic and stationary resolution was obtained at any location by OSEM with DDB only when approximate volumetric ray tracing via ray trace with multiple rays per detector bin were used. Fig. 1 shows sensitivity obtained for 16 rays per detector bin vs. a single ray trace per detector bin approach calculated for a $3 \times 3 \times 3$ pixels³ “point” source compared to experiment. The Siddon’s [ref] algorithm for the line element ray trace that was used.

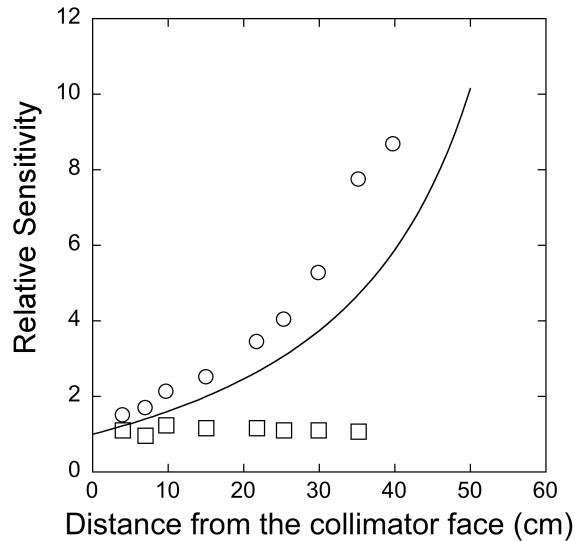


Fig. 2. Sensitivity modeling with line element ray-trace (single ray per detector unit, squares) and with volumetric ray-trace (approximated using 16 rays per detector unit, circles). Experimental data points were obtained with a cone-beam collimator (f=70 cm): solid line.

We reconstructed parallel-beam SPECT and cone-beam SPECT of Defrise phantom. The latter was reconstructed with single line element ray-tracing and with volumetric ray-tracing approximated by 16 rays per detector unit. The results are shown in Figs. 3-5.

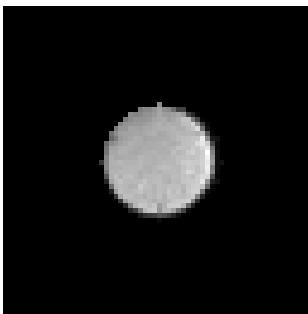


Fig. 3. Parallel-beam SPECT reconstruction of Defrise phantom (slice 33) DDB and sensitivity modeling with single ray per detector unit (line element) ray-tracing.

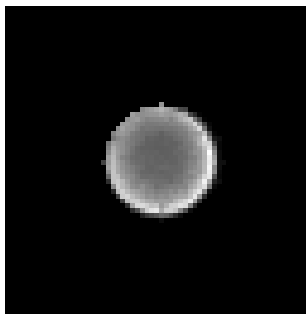


Fig. 4. Cone-beam SPECT reconstruction of Defrise phantom (slice 33) with single ray per detector unit (line element) ray-tracing and DDB and sensitivity modeling

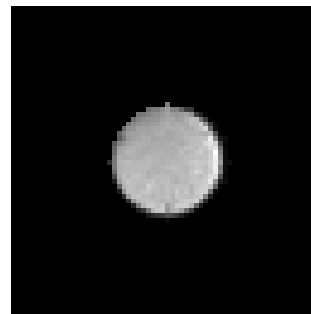


Fig. 5. Cone-beam SPECT reconstruction of Defrise phantom (slice 33) with volumetric ray-tracing, DDB and sensitivity modeling approximated using 16 rays per detector unit.

We analyzed axial and transaxial profiles obtained for Defrise phantom (Figs. 6-7). We observe that the axial profiles (i.e. number of counts in a ROI vs. slice number) obtained for reconstruction with DDB and sensitivity modeling are characterized by improved contrast and lower bias. The analysis of transaxial (i.e. within reconstruction plane) profiles indicate that in addition to DDB and sensitivity modeling, a volumetric ray-trace produced results very close to

reconstruction obtained with parallel beam collimator, while reconstruction with line element ray-trace resulted in poor quality images

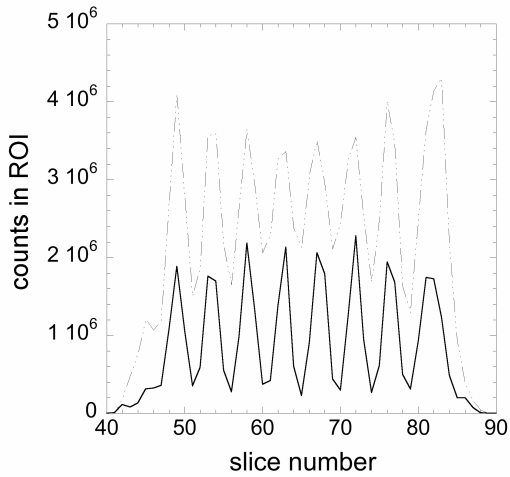


Fig. 6. Axial profiles through reconstruction of Defrise phantom cone beam SPECT shown in Figs. 2-4. CBC SPECT reconstruction, DDB, sensitivity and attenuation modeling, single ray per detector unit: dashed line; CBC SPECT, DDB, sensitivity and attenuation modeling, volumetric ray-trace approximated using 16 rays per detector unit: solid line.

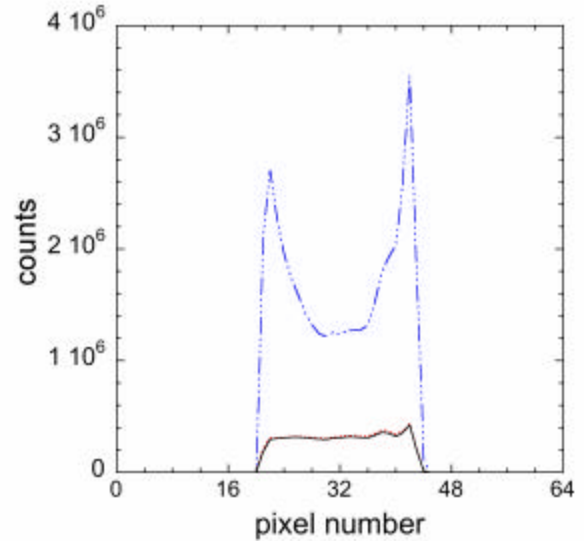
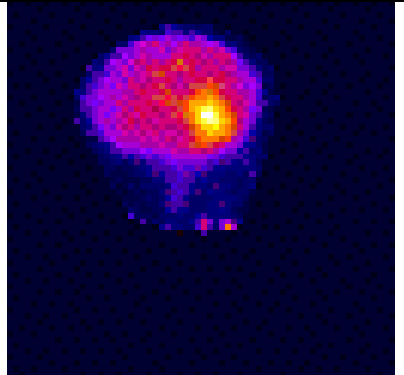
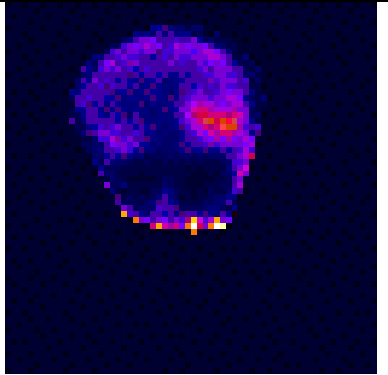
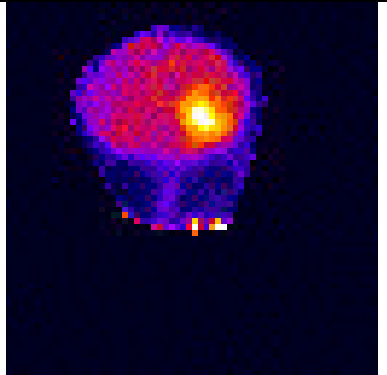


Fig. 7. Transaxial profiles through reconstruction of Defrise phantom cone beam and parallel beam SPECT (slice 33) shown in Figs. 2-4. CBC SPECT reconstruction, DDB, sensitivity, and attenuation modeling, single ray per detector unit: dashed line; CBC SPECT, DDB, sensitivity and attenuation modeling, volumetric ray-trace approximated using 16 rays per detector unit: solid line; PBC SPECT reconstruction, DDB and sensitivity modeling: dotted line.

A small number of patients with suspicious breast lesions were administered 10 mCi of Tc-99m sestamibi. SPECT Tc-99m sestamibi scintimammography (90 views, 30 sec/view) was acquired on a dual-head gamma camera (E.Cam, Siemens) with a high-resolution parallel-hole and a high-resolution cone-beam collimator. In addition, in order to simulate hot breast lesions, some patients were imaged with a number of breast skin markers each containing 1 μ Ci of Tc-99m. The tomographic images were reconstructed with DDB, sensitivity, and attenuation modeling. As in the case of the Defrise phantom, CBC SPECT data were reconstructed using a single (line-element) ray per detector unit and volumetric ray-trace approximated using 16 rays per detector unit. Examples of obtained results are shown in Figs. 8-10. We observe that CBC SPECT reconstruction with volumetric ray-trace is very similar to the reconstruction obtained for the PBC SPECT and is free of "cold" artifacts present in the CBC SPECT reconstruction with a single (line-element) ray per detector unit.

		
<p>Fig. 8. Parallel-beam breast SPECT reconstruction of a patient (slice 33) with single ray per detector unit (line element) ray-tracing.</p>	<p>Fig. 9. Cone-beam breast SPECT reconstruction of a patient (slice 33) with single (line-element) ray per detector unit ray-tracing.</p>	<p>Fig. 10. Cone-beam breast SPECT reconstruction of a patient (slice 33) with volumetric ray-tracing volumetric ray-trace approximated using 16 rays per detector unit.</p>

4. CONCLUSIONS

For a good quality fully-3D OSEM cone-beam SPECT reconstruction it is necessary to apply distance-dependent blurring and sensitivity correction, attenuation compensation, as well as volumetric ray tracing. Even if all the other corrections are applied, single ray (line element) per detector unit ray-tracing results in image artifacts. This is due to incorrect rendering of the system transition matrix. However, the volumetric ray trace requires significant increase in computer execution time and a computationally efficient approach needs to be implemented before this technique could be applied in the clinical practice.

5. REFERENCES

1. R.L. Siddon, "Fast calculation of the exact radiological path for a three-dimensional CT array", *Med. Phys.* 12(2): 252-5, 1985.
2. D.S. Lalush, B.M. Tsui, "Performance of ordered-subset reconstruction algorithms under conditions of extreme attenuation and truncation in myocardial SPECT," *J. Nucl Med.* vol. 41, pp 737-44, 2000.
3. A. Krol, I. Echeruo, R. B. Salgado, E. Lipson, J. E. Bowsher, D. H. Feiglin, F. D. Thomas. "EM-IntraSPECT Algorithm With Ordered Subsets (OSEMIS) for Non-Uniform Attenuation Correction in Cardiac Imaging", *Proceedings of SPIE*, vol. 4684, pp. 1022- 1027, 2002.
4. L.A. Shepp, Y. Vardi, "Maximum likelihood reconstruction for emission tomography," *IEEE Trans. Med. Imag.*, vol. 1, pp. 113-121, 1982.
5. K. Lange and R. Carson. "EM reconstruction algorithm for emission and transmission tomography," *J. Comp. Assist. Tomog.*, vol. 8, pp. 306-316, 1984.
6. A. Krol, J.E. Bowsher, S.H. Manglos, M.P., Tornai, D.H. Feiglin and F.D. Thomas. "An EM algorithm for estimating SPECT emission and transmission parameters from emission data only" *IEEE Trans. Med. Imaging*, vol. 20, pp. 218-232, 2001.